Available online at www.sciencedirect.com

ScienceDirect

Procedia Materials Science 4 (2014) 67 – 72

Procedia Materials Science

www.elsevier.com/locate/procedia

8th International Conference on Porous Metals and Metallic Foams, Metfoam 2013

Characterisation of ALUHAB aluminium foams with micro-CT

Norbert Babcsan[a,]*, Sandor Beke[a], Gyorgy Szamel[a], Tamas Borzsonyi[b], Balazs Szabo[b], Rajmund Mokso[c], Csilla Kadar[d], Judit Babcsan Kiss[a]

[a]*Aluinvent Zrt, Szeles u. 2, Felsozsolca H-3561 Hungary*
[b]*Institute for solid state physics and optics, Wigner research centre for physics, Hungarian academy of science, Konkoly T. M. u. 29-33., Budapest H-1121, Hungary*
[c]*Swiss Light Source, Paul Scherrer Institut, Villigen, 5232, Switzerland*
[d]*Department of materials physics, Lorand Eotvos University, Pob. 32., Budapest H-1518, Hungary*

Abstract

For quality assurance of aluminium foams the cell size determination is an important factor. Our micro-computed tomography (micro-CT) equipment is capable to image the three dimensional structure of these foams such as ALUHAB with a resolution in the range of 5-50microns. The CT parameters for the optimal image quality were determined by varying the size of the sample, the applied projection number and also the X-ray source operating parameters. The evaluation software was programmed in C language in order to determine the cell size distribution. The algorithm is capable to increase the thin cell wall contrast on the grey image and distinguish between the inner and the side cell walls, and to correct the artificial cell wall discontinuity after binarization. Future plans are to determine the distribution of the cell wall thickness, the Plateau border, the cell shape and the orientation factors.

Peer-review under responsibility of Scientific Committee of North Carolina State University

Keywords: Aluminium Foam; Properties; Structural Characterization; X-Ray Tomography; Micro-CT.

1. Introduction

Aluminium foams are cellular materials, where the 3D architecture is typically produced by foaming in the liquid state among other techniques (Banhart and Baumeister (1998)). Owing to the wide range of alloy compositions and

* Corresponding author. Tel.: +36-30-415-0001;
E-mail address: norbert.babcsan@aluinvent.com

Peer-review under responsibility of Scientific Committee of North Carolina State University
doi:10.1016/j.mspro.2014.07.598

its attractive structural and mechanical properties, ALUHAB is one of the most promising aluminium foams nowadays. The composition of its foamed composite and the special gas injection foaming method results in a very stable liquid foam having controlled and homogeneous cell size distribution. The foam is castable in this state without major structural degradation or easily machinable and processable after solidification, which makes this aluminium foam superior to the most current foams. The size of the foam cell is an important parameter, which correlates with the relative density and influences the material properties (Ashby et al. (2000)). The uniform cell size distribution is the key parameter for the application of foams (Kriszt et al. (2002)). In contrast with destructive testing methods of foams tomography is a non-invasive tool providing three-dimensional information and deep insight into the internal structure without any sample preparation. For non-destructive characterisation of foamed metals the most suitable method is tomography based on different types of radiation (Banhart (2008)). Although synchrotron generated X-ray beam could reveal even the surface structure of the cell walls, an X-ray tube with lower resolution is usually sufficient for quality control (Degischer and Kottar (1999)).

2. Experimental

2.1. X-Ray equipment

Radioscopic images of ALUHAB samples were made by a Hamamatsu L8121-03 Microfocus X-ray source, which uses an X-Ray tube with a focal spot size of 7μm, 20μm or 50μm and capable of operating at a maximum tube voltage of 150kV (Fig. 1.). For 3D tomography of the samples a Newport URS75 rotation stage was used to make appropriate number of projections. During a 360° rotation, for a proper 3D CT image, the number of projections of a sample should be at least the number of pixels in a line of the detector. In case of our high-resolution detector 2000 projections/360° should be made. We used a Hamamatsu C7942SK-25 high-resolution imaging detector, which provided a maximum image resolution of 5.4Mpixels.

2.2. Imaging

The images were grabbed through an NI PCI-1422 frame grabber board installed to a PC. Exposure, acquisition and reconstruction time, analogue integration, number of projections, detector dynamic range was properly adjusted. Radioscopic images were captured by the detector and processed through HiPic imaging software. After projection the slices were reconstructed by using Octopus 8.4 software. Its main advantages are the projection normalization, ring filter, and the reconstruction support of parallel, fan and cone beam. We applied cone beam reconstruction, which resulted in 2D slices. Using the 2D tomographic slices, open source MeVisLab 2.1 software was applied for 3D visualization. Further image processing tasks were performed in ImageJ v.1.43u software. Several parameters related to imaging and reconstruction, like utilization, contrast and noise reduction were optimized to reach the best quality images for further processing. The effect of the number of projections and the noise on the image quality is shown on Fig. 2.

3. Results and discussion

Image transformation is needed to be applied on the obtained 2D tomographic slices to make them suitable for automatic measurement and analysis of foam cell parameters. The required steps of image processing are described as follows. Fig. 3a. shows an original slice of the foam CT. In order to determine cell sizes of the foam, the grayscale images should be binarized. The binarization threshold is a critical parameter, this is demonstrated by Figs. 3b and 3c where too small and too large threshold values were applied, resulting in inadequate conversion. The proper threshold leads to accurate visualization of the cells as presented in Fig. 3d. Since the aim is to measure cell size instead of the wall parameters (solid material) the binarization (Fig. 3e) should be followed by the generation of an inverse image (Fig. 3f).

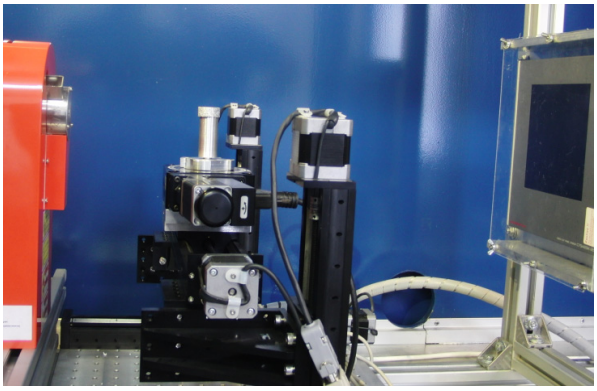

Fig. 1. Image of the applied X-Ray experimental setup.

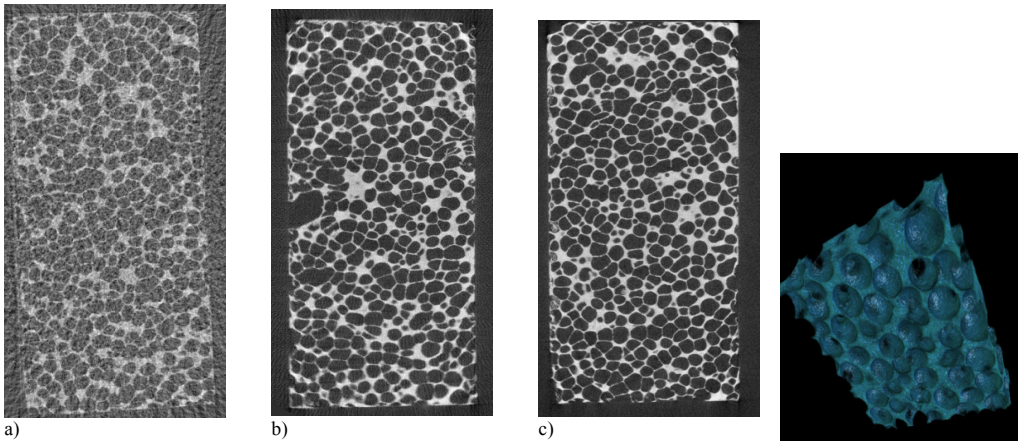

a) b) c)

Fig. 2. The effect of the number of projections on the radioscopic image quality: a; 100 projections (4 analogue integrations) b; 500 projections (4 analogue integrations) c; 2000 projections d; surface roughness on the 3D rendered image of the foam caused by noise.

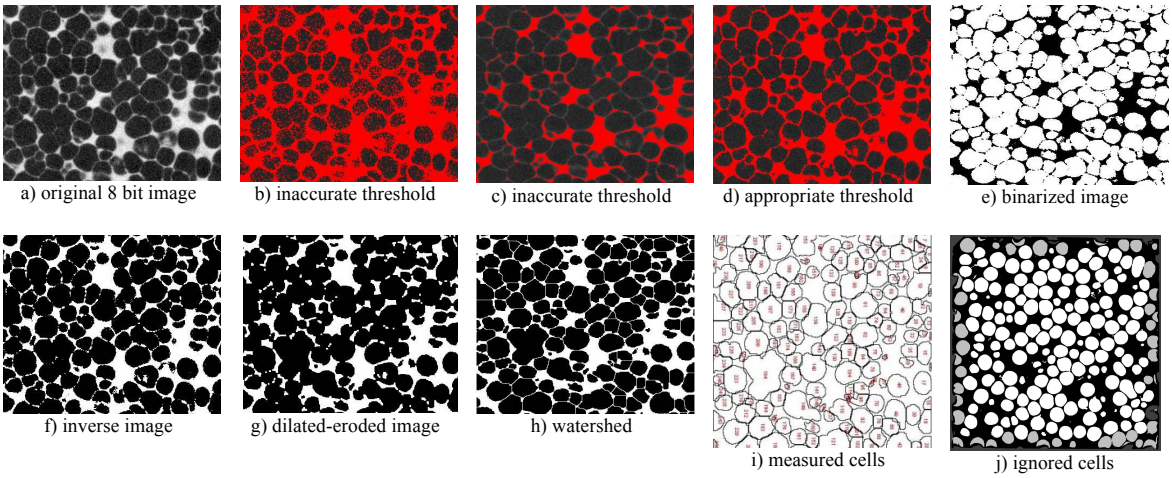

a) original 8 bit image b) inaccurate threshold c) inaccurate threshold d) appropriate threshold e) binarized image

f) inverse image g) dilated-eroded image h) watershed i) measured cells j) ignored cells

Fig. 3. Steps of image transformation.

This image shows separated cells but also cell wall discontinuities inside the cells. These defects should be hidden by dilating and eroding (Fig. 3g). The last step is watersheding (Fig. 3h), which builds up the missing parts of the walls, so the cells will be perfectly separated from each other. In this way the Image J software can distinguish individual cells and measure them in an appropriate way (Fig. 3i). During the determination of the average cell size the cell fractions at the borders of the image can cause inaccuracies. This can be eliminated by ignoring cells, which are located at a given distance from the sides (Fig. 3j). These cells (light grey coloured) are also removed from the 3D matrix.

3.1. Quantitative characterisation of the foam structure

Both 2D and 3D information can be obtained from tomographic slices. 2D analysis was performed by ImageJ, while 3D analysis was performed by Avizo Fire (VSG) and self-developed softwares of the research groups of R. Mokso (SLS, PSI, Switzerland) and T. Borzsonyi (Wigner RCP, HAS, Hungary). These softwares use different transformation parameters, filtering and algorithms to calculate the bubble size distribution histogram of the tomograms. PSI and Wigner-HAS softwares apply special watershed algorithms to identify the bubbles. The Wigner-HAS method is optimized for analyzing high-resolution tomograms (2048 x 2048 x 2048 pixels) and explodes the two phase nature of the material, as well as removes the noise originating from the tomographic reconstruction.

3.1.1. 2D IMAGE ANALYSIS

Two-dimensional image analysis was performed to determine Aluhab foam density and the average cell size distribution. Density was calculated from the ratio of solid and gas phases measured on tomographic slices (Fig. 4.).

Density values obtained by the analysis of each slice have a narrow distribution (Fig. 5.), and show a good correlation with the density value calculated from the size and weight of the foam block. Therefore the above described method is applicable to determine foam density by 2D image analysis. Assuming round cell shape, an equivalent cell diameter can be calculated for each single cell from their cross-section area values of the 2D tomography slices. Cell size distribution of an Aluhab foam block determined this way is shown on Fig. 6. For a more accurate determination of the cell size distribution, 3D image analysis is necessary.

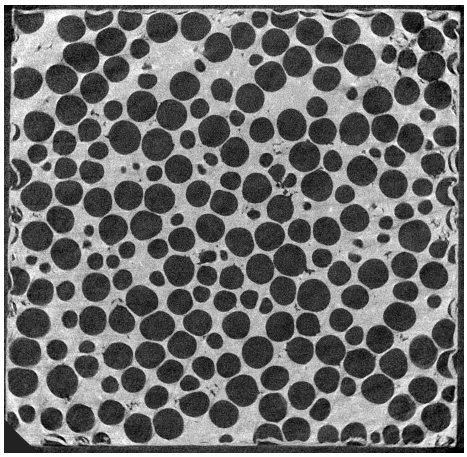

Fig. 4. 2D tomography slice of an Aluhab foam for determining the cell size distribution and the density (ρ=0.92g/cm^3).

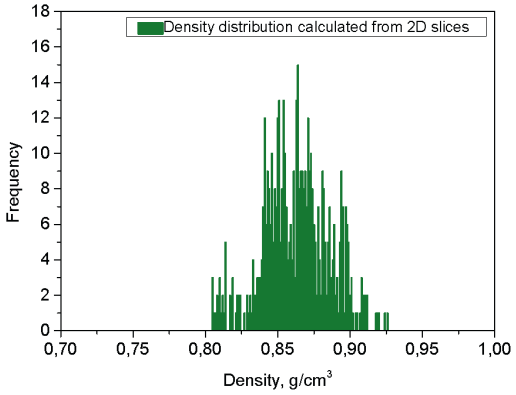

Fig. 5. The density distribution of a foam volume determined from 2D images (ρ=0.79g/cm^3).

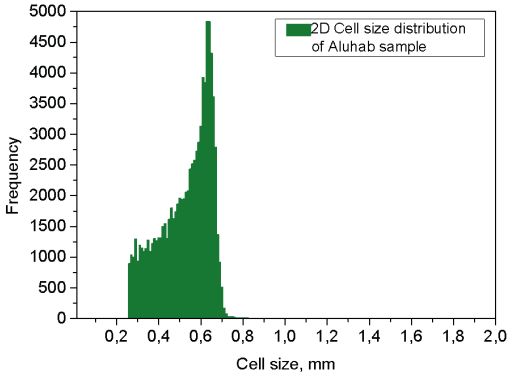

Fig. 6. Cell size distribution of Aluhab samples calculated from the data of processed 2D images of the tomography slices (ρ=0.92g/cm^3).

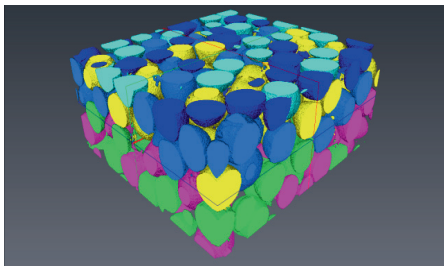

Fig. 7. Rendered 3D volume of an ALUHAB aluminium foam.

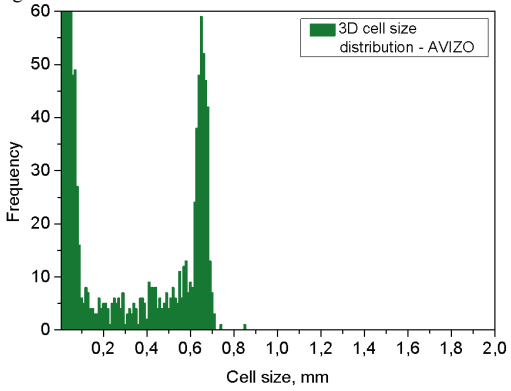

Fig. 8. The cell size distribution of Aluhab foam determined by Avizo Fire (ρ=0.92g/cm^3).

3.1.2. 3D IMAGE ANALYSIS

Rendered 3D volume section of an Aluhab aluminium foam is shown on Fig. 7. The rendered volume consists of separated whole cells and also cell fragments on the surface of the sample.

In order to investigate the effect of the cell fragments (located on the surface of the sample) on the cell size distribution, different algorithms were used. The distribution determined by Avizo Fire code has two peaks as it is shown on Fig. 8. The lower peak indicates high amount of cells below 0.1mm. The presence of bubble in the 0.15mm-0.5mm range is also assumed. The reason for the nonzero frequency between the two peaks is that cell sections on the sides of the sample have not been ignored from the analysed volume or fragmenting large cells. The distribution curve of Fig. 9. shows a peak at 0.65mm and also shows cells with diameters below 0.1mm. These cells are the results of the small cell wall discontinuities illustrated in Fig. 3g-h. The curve of the Wigner-HAS code (Fig. 10.) shows narrower cell size distribution than the other computer codes, because Wigner-HAS software does not

take into account the destroyed or deformed cells on the sample surface and also corrects for the artificial wall discontinuities resulting from finite CT resolution and binarization. The cell size distribution, hence the average cell size can be reliably determined by this computer code.

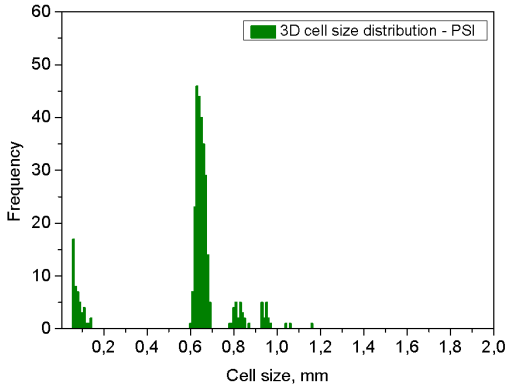

Fig. 9. Aluhab foam cell size distribution determined by algorithm of PSI (ρ=0.92g/cm^3).

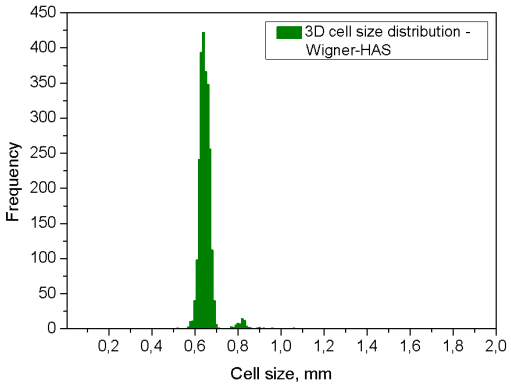

Fig. 10. Aluhab foam cell size distribution determined by algorithm of Wigner-HAS (ρ=0.92g/cm^3).

4. Conclusion

The 2D image analysis is only capable for the determination of the density distribution of the foam. Cell size distribution can be determined by 3D image analysis. However to determining the accurate cell size distribution one must not take into account the cells located on the surface, and the defects in the cell walls (like wall discontinuities) should be eliminated. Image quality, transformation parameters and handling of cell wall discontinuity have strong effect on distribution curves. CT imaging technique is an appropriate tool for non-destructive foam quality control and structural characterisation.

References

Ashby, M.F., Evans, A.G., Hutchinson, J.W., Fleck, N.A., 2000. Metal Foams: a Design Guide. Butterworth-Heinemann, USA.

Banhart, J., 2008. Advanced Tomographic Methods in Materials Research and Engineering. Oxford University Press, UK.

Banhart, J., Baumeister., J., 1998. Production Methods for Metallic Foams. MRS Proceedings 521 121–132.

Degischer, H.P., Kottar, A., 1999. On the non-destructive testing of metal foams. Metal foams and porous metal structures, ed. J. Banhart, M. F. Ashby, N. A. Fleck, MIT Press–Verlag, Germany.

Kriszt, B., Martin, U., Mosler, U., Maire, E., Degischer, H. P., Kottar, A., 2002. Characterization of Cellular Metals. Handbook of Cellular Metals: Production, Processing, Applications, eds. H.-P. Degischer and B. Kriszt, Wiley-VCH/Verlag GmbH, Germany.